AMERICAN JOURNAL OF PHYSIOLOGY
CELL PHYSIOLOGY

Am J Physiol Cell Physiol 328: C1015–C1028, 2025.
First published January 20, 2025; doi:10.1152/ajpcell.00541.2024

RESEARCH ARTICLE

Decoding Fibrosis

Role of TGF-β/SMAD/YAP/TAZ signaling in skeletal muscle fibrosis

Felipe S. Gallardo,[1,2]* Meilyn Cruz-Soca,[2]* Alexia Bock-Pereda,[2] Jennifer Faundez-Contreras,[2,3] Cristian Gutiérrez-Rojas,[2,4,5] Alessandro Gandin,[6] Veronica Torresan,[6] Juan Carlos Casar,[7] Andrea Ravasio,[8] and Enrique Brandan[2,3]

[1]*Faculty of Biological Sciences, Pontificia Universidad Católica de Chile, Santiago, Chile;* [2]*Centro Científico y Tecnológico de Excelencia Ciencia & Vida, Santiago, Chile;* [3]*Faculty of Medicine and Science, Universidad San Sebastián, Santiago, Chile;* [4]*Escuela de Kinesiología, Facultad de Ciencias, Pontificia Universidad Católica de Valparaíso, Valparaíso, Chile;* [5]*School of Medicine, Faculty of Medicine, Pontificia Universidad Católica de Chile, Santiago, Chile;* [6]*Department of Industrial Engineering, University of Padova and INSTM, Padova, Italy;* [7]*Department of Neurology, Pontificia Universidad Católica de Chile, Santiago, Chile; and* [8]*Institute for Biological and Medical Engineering, School of Engineering, Medicine and Biological Sciences, Pontificia Universidad Católica de Chile, Santiago, Chile*

Abstract

Skeletal muscle fibrosis is strongly associated with the differentiation of its resident multipotent fibro/adipogenic progenitors (FAPs) toward the myofibroblast phenotype. Although transforming growth factor type β (TGF-β) signaling is well-known for driving FAPs differentiation and fibrosis, due to its pleiotropic functions its complete inhibition is not suitable for treating fibrotic disorders such as muscular dystrophies. Here, we describe that TGF-β operates through the mechanosensitive transcriptional regulators Yes-associated protein (YAP)/ transcriptional coactivator with PDZ-binding motif (TAZ) to determine the myofibroblast fate of FAPs and skeletal muscle fibrosis. Spatial transcriptomics analyses of dystrophic and acute injured muscles showed that areas with active fibrosis and TGF-β signaling displayed high YAP/TAZ activity. Using a TGF-β-driven fibrotic mouse model, we found that activation of YAP/TAZ in activated FAPs is associated with the fibrotic process. Mechanistically, primary culture of FAPs reveals the remarkable ability of TGF-β1 to activate YAP/TAZ through its canonical SMAD3 pathway. Moreover, inhibition of YAP/TAZ, either by disrupting its activity (with Verteporfin) or cellular mechanotransduction (with the Rho inhibitor C3 or soft matrices), decreased TGF-β1-dependent FAPs differentiation into myofibroblasts. In vivo, administration of Verteporfin in mice limits the deposition of collagen and fibronectin, and the activation of FAPs during the development of fibrosis. Overall, our work provides robust evidence for considering YAP/TAZ as a potential target in muscular fibroproliferative disorders.

NEW & NOTEWORTHY The understanding of the nuclear factors governing the differentiation of muscular fibro/adipogenic progenitors (FAPs) into myofibroblasts is in its infancy. Here, we comprehensively elucidate the status, regulation, and role of the mechanotransducers Yes-associated protein (YAP)/transcriptional coactivator with PDZ-binding motif (TAZ) in the muscular fibrotic process. Our findings reveal that inhibiting cellular mechanotransduction limits FAP differentiation and the extent of muscular fibrosis exerted by transforming growth factor type β (TGF-β). This research shed new lights on the molecular mechanisms dictating the cell fate of FAPs and the muscular fibrosis.

FAPs; fibrosis; skeletal muscle; TGF-β; YAP/TAZ

INTRODUCTION

Muscular dystrophies are a diverse group of myopathies mainly manifested by the loss of critical proteins connecting the myofiber to the surrounding extracellular matrix (ECM). Mutations affecting the production of the cytoskeleton-associated scaffolding protein dystrophin result in the development of Duchenne muscular dystrophy (DMD), the most common and severe dystrophic type (1). Due to contraction movements, myofibers undergo constant degeneration, leading to the buildup of a chronic inflammatory environment. Several cytokines released by inflammatory cells affect the native behavior of resident stromal cells, ultimately promoting the accumulation of a disorganized ECM that affects the architecture and performance of the tissue, a process known as the fibrotic response.

Fibrosis is recognized to be triggered by the dysregulated activation of tissue-resident fibroblasts/stromal cells and

*F. S. Gallardo and M. Cruz-Soca contributed equally to this work.
Correspondence: E. Brandan (enrique.brandan@uss.cl).
Submitted 29 July 2024 / Revised 22 August 2024 / Accepted 31 January 2025

their conversion into highly contractile ECM-producing myofibroblasts (2). Fibro/adipogenic progenitors (FAPs) are the multipotent fibroblasts/stromal cell population of the skeletal muscle characterized by the expression of platelet-derived growth factor receptor α (PDGFRα). Activated FAPs accumulate in the fibrotic ECM and contribute to this environment by expressing large quantities of ECM molecules (3–5). One of the most recognized stimuli driving both FAPs differentiation and muscular fibrosis is the signaling of the transforming growth factor type β (TGF-β) (3, 6–8).

TGF-β belongs to the TGF-β superfamily of growth factors that signal through a heterotetrameric serine/threonine kinase receptor complex [containing TGF-β receptors I and II (Tβ-RI and -RII)], which induces the activation, through phosphorylation, of the single mediator of the pathway, the mothers against decapentaplegic (SMAD2/3 in the case of TGF-β subfamily) transcription factors (TFs) (9). Once activated, phospho-SMAD2/3 can, in turn, form a ternary complex with the nonreceptor-activated SMAD4 and translocate to the nucleus. The complex binds to specific SMAD binding elements (SBE) on the promoter sequences of TGF-β-regulated genes to orchestrate gene expression programs. Mammals express three TGF-β isoforms (TGF-β1, -2, and -3), and all of them are upregulated in fibrotic muscle with the faculty to induce genes associated with the myofibroblast phenotype in FAPs (6). Thus, understanding FAPs biology and TGF-β profibrotic signaling mechanisms is critical for comprehension of the underlying pathophysiology of muscular dystrophies and the fibrotic response.

The paralogous transcriptional coregulators Yes-associated protein (YAP) and transcriptional coactivator with PDZ-binding motif (TAZ), hereafter YAP/TAZ, emerges as a promising actionable target in skeletal muscle fibrosis (10). YAP/TAZ operates in the nucleus, where it interacts mainly with members of the transcriptional enhancer factor (TEA)-domain (TEAD) family of TFs to control the expression of a set of genes, providing the potential to regulate pivotal biological processes such as proliferation, cell fate specification, and tissue growth. Over the years, the regulation of YAP/TAZ has often been overlooked, with the primary focus on its suppression by the tumor suppressor Hippo pathway. This regulation occurs through inhibitory phosphorylation, leading to cytoplasmic sequestration and subsequent degradation. Nevertheless, various modulators, some even overriding the Hippo pathway, have been identified. YAP/TAZ function as highly conserved molecular mechanotransducers, responding to the cell's mechanical state and shape (11). For instance, YAP/TAZ is activated when cells experience sufficient actomyosin-cytoskeleton tension due to cell spreading and the sensing of high ECM stiffness and adhesiveness (12–14).

YAP/TAZ can interact with SMADs, dictating their nuclear localization and transcriptional activities (15–19). Thus, YAP/TAZ loss of function suppresses fibrosis in several organs and affects myofibroblast differentiation of their corresponding fibroblasts/stromal cells induced by TGF-β (10, 20–24). Regarding skeletal muscle, expression of a constitutively active form of YAP in a healthy mouse induces features of muscular dystrophy such as myofiber necrosis, myogenesis, atrophy, and fibrosis (25, 26). Moreover, we have previously demonstrated the induction of YAP/TAZ activity in denervated muscles (an experimental model of muscle fibrosis), and also that FAPs activate YAP/TAZ in response to the profibrotic signaling lipid lysophosphatidic acid (27, 28). Here, we show the conserved ability of YAP/TAZ to determine cell fate decisions of muscular FAPs in response to TGF-β signaling, ultimately affecting the development of muscular fibrosis. Using different YAP/TAZ inhibitors (affecting at the nuclear and mechanosensing level), we showed that YAP/TAZ is critical for allowing the differentiation of FAPs in vitro and the development of fibrosis in vivo. Moreover, we provide spatial omics analyses indicating that the activities of YAP/TAZ and TGF-β correlate and are spatially associated in the fibrotic muscle. This work proposes YAP/TAZ as a potential actionable target for muscular dystrophies.

MATERIALS AND METHODS

Animal Experiments

Animal procedures were reviewed and approved by the Animal Ethics Committee of Fundación Ciencia & Vida (P065/2024). PDGFRα^{EGFP} (JAX Stock No. 007669) (29) and mdx (JAX Stock No. 001801) mice were housed before and during experiments in adequate cages, in groups of 4 animals/cage, with a 12-h light-dark cycle, and fed ad libitum. For induction of fibrosis, 5-mo-old male PDGFRα^{EGFP} mice (25–30 g) were anesthetized with 2%–3% isoflurane gas in oxygen at a rate of 0.2 L/min. Animals' limbs were shaved and aseptically treated with 2% chlorhexidine. A solution containing 50% vol/vol glycerol and 20 ng/μL of human recombinant TGF-β1 (240-B, R&D) dissolved in 50 μL phosphate buffered solution (PBS) was injected in the left tibialis anterior. As a control, the contralateral (right) muscle in the same animal was injected with 50 μL of PBS. Verteporfin (SML0534, Sigma-Aldrich) was prepared as originally suggested (30). Mice received 50 mg/kg of Verteporfin intraperitoneally every 2 days (4 doses), beginning on the same day but 8 h before recombinant human TGF-β1 dissolved in glycerol (G + Tβ) injection. Animals were monitored for potential suffering every other day, and analgesia was delivered with 30 mg/kg of tramadol administered orally. Mice were euthanized after 7 days of G + Tβ injection by cervical dislocation, and tibial anterior muscles were collected and snap-frozen in liquid nitrogen-cooled isopentane.

FAPs Isolation and Cell Culture

Isolation of primary muscular FAPs was based on an adhesion protocol using a preplating method previously described (3, 28). Briefly, hindlimb muscles from C57Bl/6j (JAX Stock No. 000664) mice were collected, cleared from adipose tissue and tendons, and mechanically minced. Small pieces were then subjected to enzymatic digestion at 37°C with 25 mg/g muscle of Collagenase/Dispase (COLLDISP-RO, Roche) dissolved in high-glucose Dulbecco's modified Eagle's medium (DMEM) (12800017; Gibco). After 45 min agitation, the suspension was filtered through 70-μm cell strainers, pelleted, resuspended in DMEM supplemented with 10% fetal bovine serum (FBS) (SH30071.02, Hyclone) and antibiotics (P4333, Sigma-Aldrich), and incubated on 10-cm dishes at 37°C, 5% CO_2, and 95% humidity. After 90 min, the medium was refreshed to remove nonadherent cells. Primary cells were used up to *passage 2*, associated with loss of PDGFRα

expression (3). C3H/10T1/2 cells (CCL-226, ATCC) were maintained and treated identically as FAPs.

For treatments, FAPs were stimulated for the indicated times and concentrations with TGF-β1 in DMEM supplemented with 1% FBS. The SMAD3 inhibitor SIS3 (6 μM; 1009104-85-1, Merck Calbiochem) and the Tβ-RI inhibitor SB525334 (10 μM; S8822, Sigma-Aldrich) were added right before TGF-β addition. Verteporfin (0.2 μM) and the Rho inhibitor I C3 (2 μg/mL; CT04, Cytoskeleton, Inc.) were added 2 h before TGF-β addition. All inhibitors were dissolved in dimethyl sulfoxide (DMSO), also used as vehicle control.

Protein Extraction, SDS-PAGE, and Western Blot

Protein expression analyses from whole muscle extracts and cells were performed as described previously (27, 28). In brief, equal amounts of proteins were electrophoretically separated and blotted onto Immobilon-P PVDF membranes (IPVH00010, Millipore). Membranes were blocked with 5% nonfat milk in Tris-buffered saline-Tween 20 (TBST) buffer (50 mM Tris-HCl pH 7.6, 150 mM NaCl and 0.1% Tween 20) and incubated with the following antibodies: anti-YAP/TAZ 1:1,000 (8418, CST), anti-Fibronectin 1:2,000 (F3648, Sigma-Aldrich), anti-Transcription factor 4 (TCF4) 1:1,000 (2569S, Cell Signaling Technology), anti-PDGFRα 1:1,000 (AF1062, R&D), anti-β1-Integrin 1:1,000 (sc-8978, Santa Cruz Biotech.), and anti-GAPDH 1:2,000 (sc-365062, Santa Cruz Biotech.). Chemiluminescence was generated using horseradish peroxidase (HRP)-conjugated secondary antibodies and SuperSignal Luminol/Enhancer substrates (Thermo Scientific). ImageJ software (v.1.53k, NIH) was used to obtain pixel density values and produce quantifications.

RNA Extraction and RT-qPCR

RNA from muscle was extracted using TRIzol according to the manufacturer's instructions. Either TRIzol or E.Z.N.A. Kit Total RNA (R6834, Omega Bio-Tek) was used for cells. RNA was reversed-transcribed into complementary DNA, and quantitative PCR was performed in duplicate using PowerUp SYBR Green master mix (A25741, Applied Biosystems) on an Eco Rea-Time (Illumina) or QuantStudio 3 Real-Time (Thermo Scientific) PCR systems. The following primer sets (Integrated DNA Technologies) were used: *Ankrd1* (F: 5′-GGA TGT GCC GAG GTT TCT GAA-3′ and R: 5′-GTC CGT TTA TAC TCA CAG AC-3′), *Cyr61* (F: 5′-TAA GGT CTG CGC TAA ACA ACT C-3′ and R: 5′-CAG ATC CCT TTC AGA GCG GT-3′), *Ctgf* (F: 5′-CAG GCT GGA GAA GCA GAG TCG T-3′ and R: 5′-CTG GTG CAG CCA GAA AGC TCA A-3′), *Tagln2* (AGC AGA TCC TCA TCC AGT GG-3′ and R: 5′-CCA TCT GCT TGA AGG CCA-3′), *Acta2* (F: 5′-TCC CTG GAG AGG AGC TAC GA-3′ and R: 5′-CTT CTG CAT CCT GTC AGC AA-3′), and *Gapdh* (F: 5′-TGA CAT CAA GAA GGT GAA G-3′ and R: 5′-TCC TTG GAG GCC ATG TAG GCC AT-3′). The comparative $2^{-\Delta\Delta Ct}$ method was used to determine mRNA expression.

Staining and Immunofluorescence

Sirius red staining was done as described previously (31). Sections were imaged with a Leica DMi8 microscope. Images were segmented and positive area was quantified using ImageJ. Immunofluorescence was carried out as previously described for cells (28) and tissue sections (27). The following antibodies were incubated overnight at 4°C in blocking buffer (PBS, 1% bovine serum albumin): anti-YAP/TAZ 1:150 (8418, CST), anti-Fibronectin 1:500 (F3648, Sigma-Aldrich), and anti-α-SMA 1:250 (A2547, Sigma-Aldrich). Hoechst 1 mg/mL and Alexa Fluor 568 Phalloidin 1:500 (A12380, Invitrogen) were used to stain nuclei and F-actin, respectively. Samples were imaged using an LSM 880 ZEISS confocal microscope with Airyscan detector (Fig. 2, *E* and *H* and Fig. 3*D*), a Nikon Eclipse E600 microscope (Fig. 2*B*, Fig. 3*B*, and Fig. 4, *A* and *C*), and a Leica DMi8 microscope (Fig. 5, *B*–*D*).

For YAP/TAZ intensity analysis (Fig. 3*H*), the green channel corresponding to the enhanced green fluorescent protein (EGFP) signal (FAPs nucleus) was converted to 8-bit format, blurred with a Gaussian filter (sigma = 2.0), segmented, analyzed for particles, and added to ROI Manager. Then, signal intensity was measured in the YAP/TAZ channel within every segmented EGFP+ nuclei and normalized to the intensity of the whole image. Quantification of the fibronectin area and the number of EGFP positive nuclei was performed similarly to YAP/TAZ analysis. Briefly, after segmentation, the fibronectin-positive area was calculated as the percentage of pixels above the given threshold. For EGFP nuclei, the number of identified particles positive above the given threshold was counted. As stated in the text, for a better visualization, EGFP images from G + Tβ muscles were presented with an increased intensity. All analyses were performed using the original intensity of the image, i.e., same acquired intensity as images from the control muscles. Counting of cells with α-SMA stress fibers (Fig. 4*A*) was done by a blind operator. The instruction was to count cells with cable-like structures spanning the whole cell body. The percentage of positive cells was calculated based on the total number of cells per field.

Hydrogels Preparation

Polyacrylamide (PAA) substrates were prepared as documented by Gandin et al. (32). Briefly, a pre-mix PAA solution containing acrylamide (AA), bis-acrylamide (BA), and *N*-hydroxyethyl acrylamide (HEAA; 697931, Sigma-Aldrich) was prepared. Soft hydrogels contained 3.5% AA, 0.03% BA, and 2.3% HEAA, whereas stiff hydrogels contained 6.6% AA, 0.48% BA, and 2.3% HEAA. PAA solution was degassed for 20 min, and 1% ammonium persulfate and 0.1% tetramethylethylenediamine were added for polymerization. The polymerizing solution was quickly poured into polydimethylsiloxane (PDMS) rings (20 mm diameter and 0.3 mm height) placed on Kapton tape. Rings were sealed on top with a 25-mm dried coverslip previously incubated with NaOH for 3 min, (3-aminopropyl)trimethoxysilane for 3 min, and 0.5% glutaraldehyde for 30 min. Polymerized hydrogels were removed from PDMS rings, placed on culture wells, washed three times with PBS, and exposed to UV for 15 min. Hydrogels were functionalized with 25 μg/mL of fibronectin at 37°C overnight (sc-29011, Santa Cruz Biotech). Cells were seeded in a drop and treated with TGF-β after 24 h of growth on hydrogels.

Spatial and Single-Cell Transcriptomics

Spatial transcriptomics (33) and single-cell RNA-seq (34) data were downloaded from Gene Expression Omnibus

(GEO) under the accession codes GSE225766 (Supplemental File: GSE225766_RAW.tar) and GSE213925 (Supplemental File: GSE213925_RAW.tar), respectively. Data were analyzed in R and with the Seurat package (v.4.2.1).

For spatial data, matrices were SCTransformed and subjected to standard Seurat workflow (FindNeighbors dims = 1:30; FindClusters resolution = 0.6; RunUMAP dims = 1:30). For single-cell data, high-quality cells containing less than 15% expressed genes mapped for mitochondrial origin and between 500–5,000 (wild type, WT) or 800–6,000 (mdx and mdxD2) expressed genes were maintained. Matrices were merged, normalized, and then integrated using the "IntegrateData" function with default settings. Seurat standard workflow was followed to scale the data and run dimensionality reductions by principal component analysis (PCA) and uniform manifold approximation and projection (UMAP; dims = 1:5). Cell clusters were identified using "FindNeighbors" (dims = 1:5) and "FindClusters" (resolution = 0.2) functions. FAPs cluster, determined by the expression of Pdgfra, was subset and cells were separated into Vcam1/Adam12-expressing cells (Vcam1 & Adam12 levels > 0.2) and remaining cells (Vcam1 & Adam12 levels < 0.2). The subset matrix was subjected to a second round of integration, normalization, scale, and reduction by PCA.

Signatures scores for each cell (single cell) and spot (spatial) was determined by calculating the average expression of the sum of values of all the genes contained in the respective signature. YAP/TAZ and TGF-β signatures were from Alsamman et al. (35) and Padua et al. (36), respectively. FAPs signature was created using the top 20 genes expressed by FAPs by Saleh et al. (34) (Supplemental data: 'Table S2'). Fibrosis score was the average expression value of fibronectin (Fn1) and Col1a1 together, and plots were created using the SpatialFeaturePlot function (min.cutoff = 'q10').

Statistical Analysis

All graphs show mean and standard deviation unless otherwise indicated. Biological replicates are illustrated as dots within each graph and indicated in the figure legend. Statistical difference was considered with a P value less than 0.05. Comparisons between one variable (e.g., treatment) or two variables (e.g., treatment plus inhibitor) were performed using unpaired t test or two-way ANOVA, respectively. When two-way ANOVA was required, Bonferroni's multiple comparisons test was done. Graphs and statistical analysis were obtained using Prism 9 for MacOS software (v.9.5.1).

RESULTS

High YAP/TAZ Activity Is Spatially Associated with Fibrotic Environments with High TGF-β Signaling

Other groups and we have demonstrated that YAP/TAZ is dysregulated in fibrosis-affected muscles (26, 27, 37). For example, muscle denervation triggers fibrosis and YAP/TAZ upregulation (26, 27). However, dystrophic muscles are far from being as homogeneous as denervated muscles, and indeed they are characterized by restricted tissue foci, where myofiber rupture, fibrosis, and regeneration occur among the immediate healthy surroundings. We expected that if YAP/TAZ is integral to fibrosis, we could be able to detect increased YAP/TAZ signature mapping preferentially in fibrotic-damaged zones. In support of this idea, our laboratory has also shown, through laser microdissection of mdx muscle, that one of the most recognized YAP/TAZ target genes, connective tissue growth factor (CTGF, also known as CCN2), is highly expressed in zones of active muscle damage and regeneration (38). Thus, to spatially resolve the YAP/TAZ status, we analyzed published spatial transcriptomics of muscle from an animal model of DMD, the mdxD2 mouse (a severe mdx on the DBA/2J genetic background) (Fig. 1*A*, *top*) (33). Inspection of districts with high fibrosis (fibronectin and collagen 1 levels) (Fig. 1*B*) and unsupervised clustering (Fig. 1*C*) efficiently revealed that the spots clustered as number 3 correspond to clear areas of active damage and fibrosis. We compute the activity of YAP/TAZ by analyzing the level of a 151-gene signature (expression of YAP/TAZ target genes). Expectedly, cluster 3 exhibited high YAP/TAZ activity when compared with the rest of spots (Fig. 1*D*). To add robustness to our finding and expand beyond muscular dystrophies, we leveraged the spatial activity of YAP/TAZ during acute muscle regeneration in which fibrosis transiently occurs (Fig. 1*A*, *bottom*). Same as with mdxD2 muscles, we found that clusters 4 and 9 represent reliable fibrotic environments with high YAP/TAZ activity (Fig. 1, *B–D*, *bottom*). Then, to uncover the cellular and molecular determinants of YAP/TAZ activation in these fibrotic foci, we focus on the well-recognized fibrotic driver pair; FAPs and TGF-β signaling. Exploration of TGF-β and FAPs signatures (34, 36) revealed that both signatures are also increased in fibrotic zones and show a high degree of correlation with YAP/TAZ activity (Fig. 1, *D–F*). These observations placed YAP/TAZ as an integral element of fibrotic muscle and a valuable tool for exploration.

TGF-β-Rich Injury Induces YAP/TAZ Activity in Skeletal Muscle

To investigate whether TGF-β can effectively induce YAP/TAZ activation in muscle in vivo, we injected recombinant human TGF-β1 dissolved in glycerol (G + Tβ) into the tibialis anterior muscle of healthy mice (Fig. 2*A*). The addition of TGF-β to glycerol inhibits adipogenesis while promoting fibrogenesis (39). We found a significant fibrotic response determined by increased collagen and fibronectin deposition (Fig. 2, *B* and *E*). We assessed the activation of YAP/TAZ in these mice by levels of protein and the expression of its classic target genes. Fibrosis derived from this experimental model was associated with an upregulation of YAP/TAZ and its target genes *Ankrd1*, *Cyr61*, *Ctgf*, and *Tagln2* (Fig. 2, *C* and *D*). Then, to investigate the contribution of FAPs, we took advantage of the PDGFRα^{EGFP} knock-in mouse (29). In this mouse, EGFP is driven by the activity of the PDGFRα promoter (main FAPs marker) and thus, the levels of EGFP expression can be used as a readout of PDGFRα status. Importantly, downregulation of PDGFRα is connected to the differentiation of FAPs into myofibroblasts in response to TGF-β (Supplemental Fig. S1A) (40). As expected, G + Tβ induced a massive expansion of FAPs (Fig. 2, *E* and *F*) coupled with a huge reduction of the EGFP signal in each cell (Fig. 2*G*), indicating the activation of FAPs. For the sake of visualization of EGFP cells, from now on we present images of EGFP from the G + Tβ muscle with increased intensity. Thus, to monitor whether increased

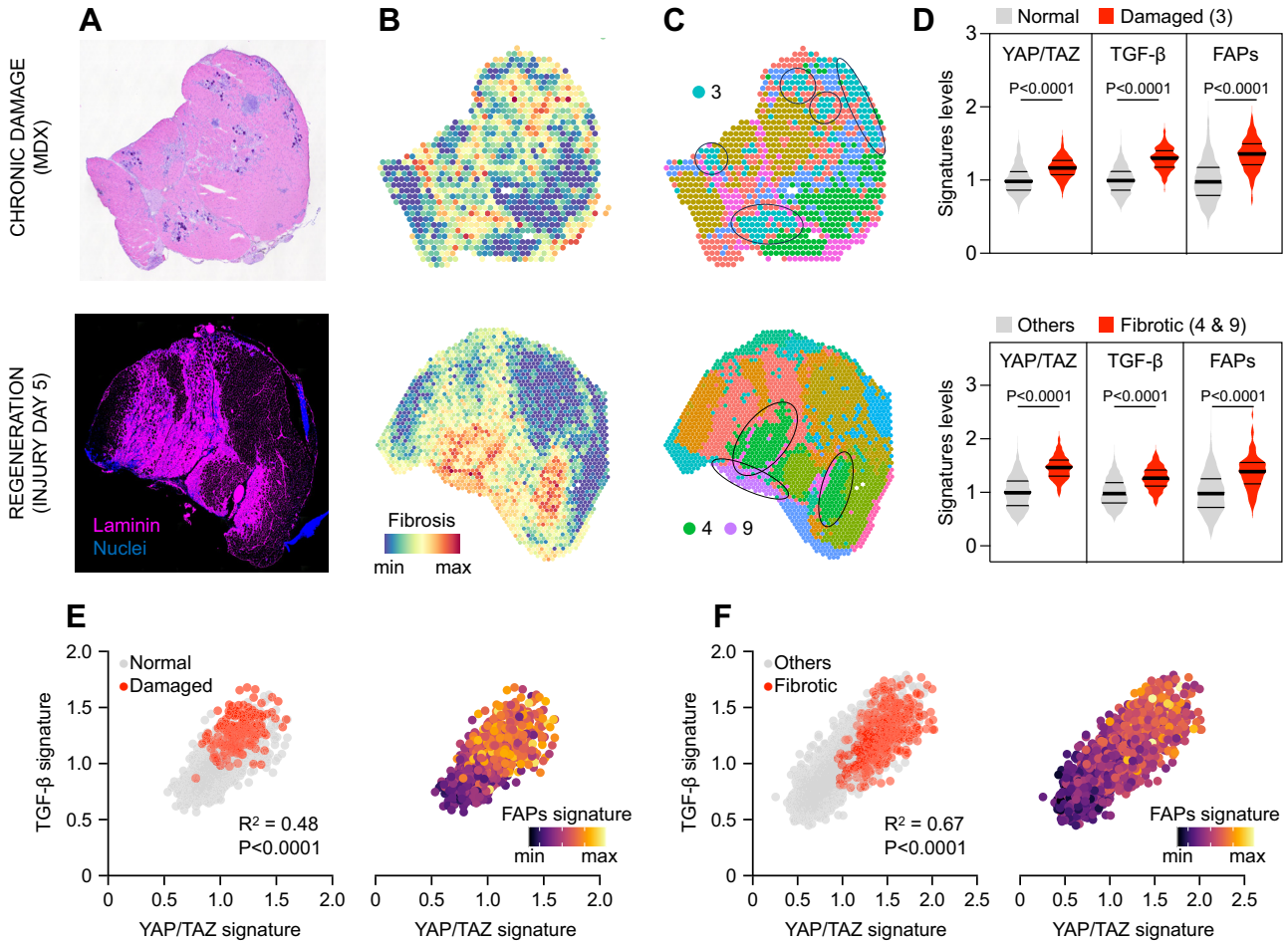

Figure 1. Yes-associated protein (YAP)/transcriptional coactivator with PDZ-binding motif (TAZ) activity spatially accumulates in fibrotic environments with high transforming growth factor type β (TGF-β) signaling and fibro/adipogenic progenitors (FAPs) accumulation. *A*: original images of dystrophic [*top*; hematoxylin-eosin (H&E) staining] and injured (*bottom*; immunostaining) muscles used for spatial sequencing. Images reproduced with permission from Michael Stec (33). *B* and *C*: feature plot of fibrosis abundance (*B*) and plot of unsupervised clustering (*C*). *D*: violin plots representing YAP/TAZ, TGF-β, and FAPs signatures levels in normal (gray violins) or damaged and fibrotic (red violins) spots. *E* and *F*: correlation analysis between YAP/TAZ, TGF-β, and FAPs signatures levels in mdx (*E*) and injured (*F*) muscles.

expression of YAP/TAZ is associated with FAPs differentiation we performed immunostaining against YAP/TAZ and segmented FAPs nuclei into two categories corresponding to EGFP^{high} ('resting') FAPs and EGFP^{low} ('activated') FAPs (Fig. 2, *H* and *I*). Analysis of a total of 3,167 nuclei coming from both control and G + Tβ muscles indicated that while 'resting' EGFP^{high} FAPs are equally derived from normal and damaged muscles, 'activated' EGFP^{low} FAPs are exclusively found in G + Tβ-injured muscles (Fig. 2*I*). With this in mind, we determined the nuclear YAP/TAZ signal of each nucleus in the two groups. Strikingly, Fig. 2*J*, *left*, shows that 'activated' FAPs have increased YAP/TAZ signal compared with 'resting' FAPs. Moreover, since G + Tβ muscles were enriched in EGFP^{low} FAPs, an average value of the YAP/TAZ intensity per each muscle also increased during damage (Fig. 2*J*, *right*). All in all, these data indicate that in vivo, the differentiation of FAPs into myofibroblasts is coupled with an increased in YAP/TAZ expression, suggesting a contribution to the overall activation of YAP/TAZ at whole tissue level. Thus, YAP/TAZ is highly activated during the muscle repair process involving strong TGF-β signaling.

The Canonical TGF-β/SMAD Pathway Drives YAP/TAZ Activation in FAPs

Our previous data indicate a strong association between TGF-β signaling and YAP/TAZ activity, motivating us to monitor the direct influence of TGF-β over YAP/TAZ in FAPs. We performed a primary culture of these cells using a plating method originally described to isolate muscular TCF4+ fibroblasts (Fig. 3*A*) (41). Our laboratory has previously described the indistinguishable overlap between TCF4+ fibroblasts and PDGFRα+ FAPs and thus considered them as the same cell identity (3). Indeed, the isolation of FAPs from the PDGFRα^{EGFP} mouse using this plating method further validated our culture specificity since nearly all cells in the culture were nuclear EGFP positive (Fig. 3*B*). To corroborate our findings in primary cell culture, we also used the nonmuscle embryonic mesenchymal cell line C3H/10T1/2, which behaves identically to FAPs in response to TGF-β (Supplemental Fig. S1A) (40, 42).

To investigate the effects of TGF-β1 over YAP/TAZ in FAPs, we first analyzed the expression of YAP/TAZ target

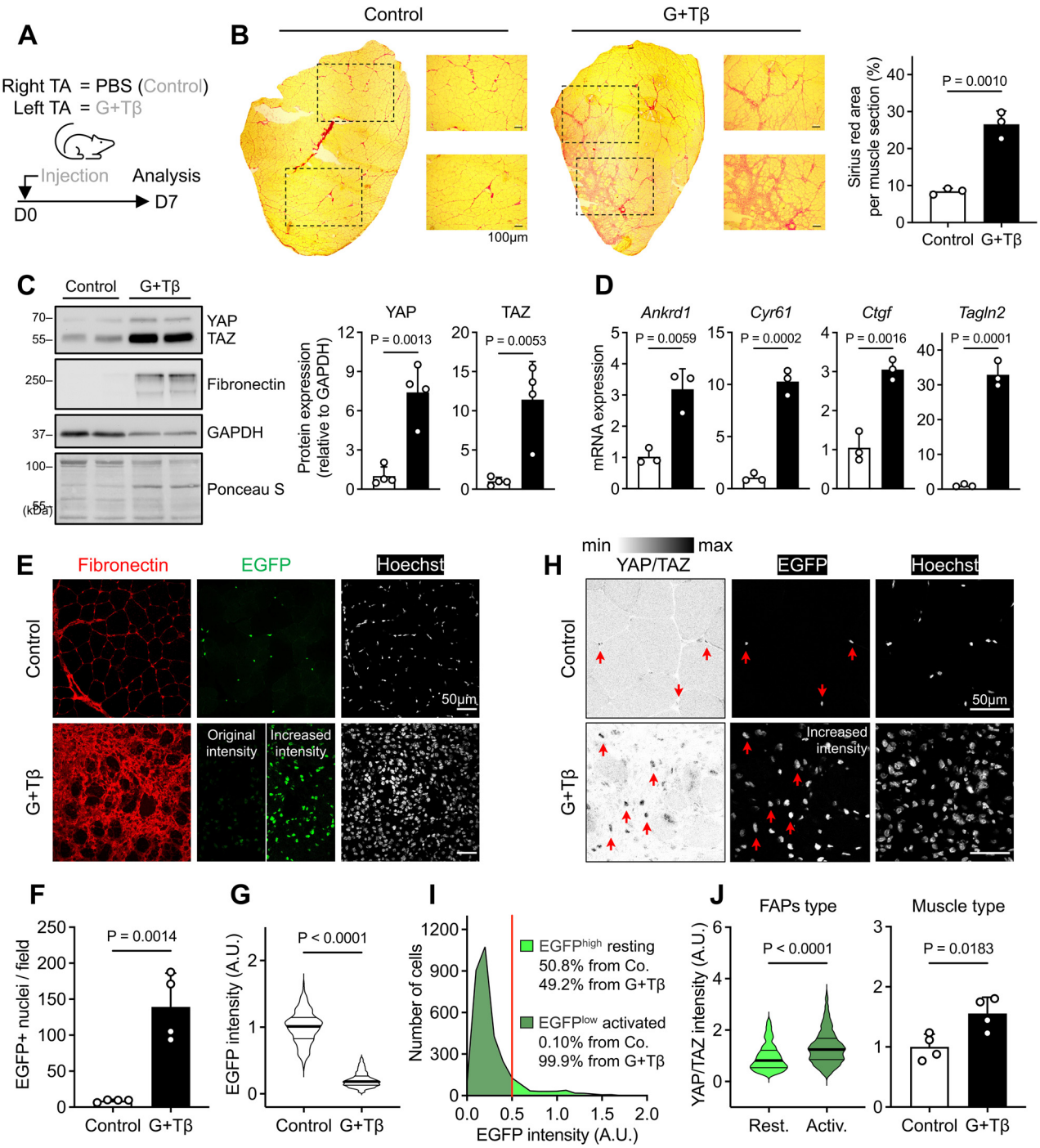

Figure 2. Fibrotic skeletal muscles induced by recombinant human transforming growth factor type β (TGF-β1) dissolved in glycerol (G + Tβ) injection show augmented Yes-associated protein (YAP)/transcriptional coactivator with PDZ-binding motif (TAZ) activity in activated fibro/adipogenic progenitors (FAPs). *A*: illustration of the conditions and temporality of the G + Tβ model. *B*: representative sections from muscles as in *A* stained with Sirius red for collagen visualization. *Right*: quantification of Sirius red positive area. $n = 3$ independent mice. *C*: representative Western blot for YAP/TAZ expression from muscles as in *A*. Fibronectin was used as fibrotic control. *Right*: quantification of YAP/TAZ expression relative to GAPDH levels. $n = 4$ independent mice. *D*: RT-qPCR analysis showing expression levels of YAP/TAZ target genes from muscles as in *A*. $n = 3$ independent mice. *E*: representative images from muscles as in *A* showing fluorescence signals for fibronectin (red), nuclei of FAPs (enhanced green fluorescent protein, EGFP), and total nuclei (gray). Increased intensity is used for better visualization of EGFP positive nuclei. *F*: quantification of the number of FAPs per field from images in *E*. $n = 4$ independent mice. *G*: single-cell quantification of the EGFP intensity in FAPs from images in *E*. $n = 187$ (Control) and 2,851 (G + Tβ) nuclei pooled from four independent mice. *H*: representative images of muscles as in *A* showing fluorescence signals for YAP/TAZ (inverted grayscale), nuclei of FAPs (EGFP; grayscale), and nuclei (grayscale). Red arrows indicate overlap between YAP/TAZ and EGFP signals. *I* and *J*: distribution of cells based on EGFP intensity from muscles as in *A*. Red line crossing *x*-axis indicate threshold for FAPs segmentation (activated < 0.5 > resting). $n = 3{,}167$ total nuclei. *J*, *left*: single-cell quantification of the YAP/TAZ intensity within resting (Rest.) and activated (Activ.) FAPs from images in *H*. $n = 352$ (Rest.) and $n = 2{,}764$ (Activ.) nuclei pooled from four independent mice. *Right*: average YAP/TAZ intensity from EGFP nuclei per each muscle. $n = 4$ independent mice.

AJP-Cell Physiol • doi:10.1152/ajpcell.00541.2024 • www.ajpcell.org

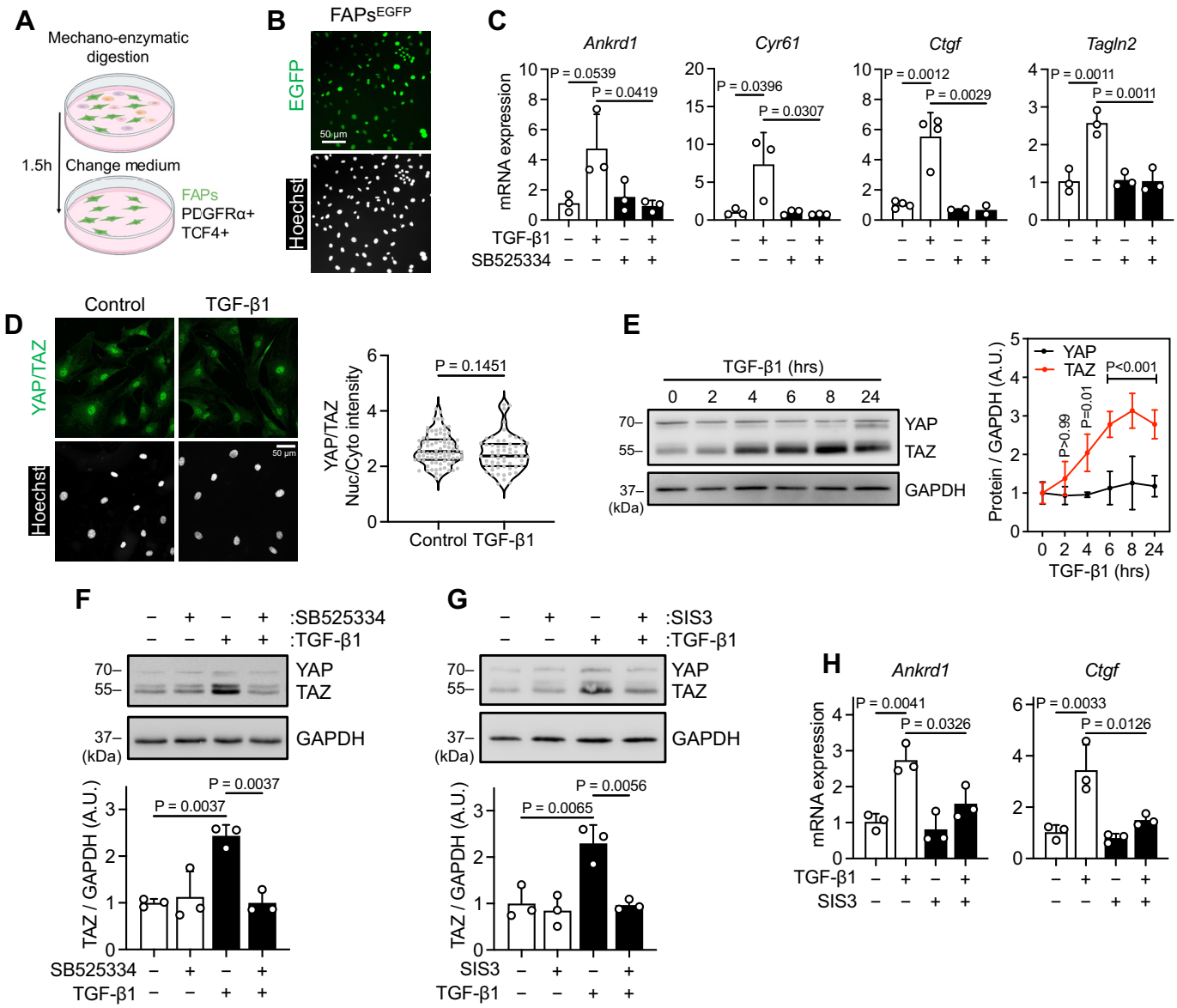

Figure 3. Transforming growth factor type β (TGF-β) signaling activates Yes-associated protein (YAP)/transcriptional coactivator with PDZ-binding motif (TAZ) in fibro/adipogenic progenitors (FAPs) through canonical SMAD3. *A*: illustration showing the preplating strategy for isolation of muscular FAPs (platelet-derived growth factor receptor α, PDGFRα/TCF4 positive cells). *B*: fluorescence images showing nuclear enhanced green fluorescent protein (EGFP) (EGFP:H2B) expression in isolated FAPs from the PDGFRα^{EGFP} mouse. Hoechst was used to visualize all cells. *C*: RT-qPCR analysis showing expression levels of YAP/TAZ target genes from FAPs treated with or without 5 ng/mL TGF-β (24 h) and in the presence or absence of the TGF-β receptor I (Tβ-RI) inhibitor SB525334. $n = 3$–4 independent experiments. *D*: immunofluorescence images showing YAP/TAZ localization in FAPs treated with or without 1 ng/mL TGF-β1 for 24 h. *Right*: quantification of nuclear/cytoplasmic ratio of YAP/TAZ signal intensity. $n = 85$ (Control) and $n = 60$ (TGF-β1) cells pooled from two independent experiments. *E*: Western blot displaying YAP/TAZ expression in FAPs treated with 5 ng/mL TGF-β1 for the indicated times. *Right*: quantification of YAP/TAZ expression relative to GAPDH levels. $n = 3$ independent experiments. Statistical comparison were to 0 h of TGF-β1. *F* and *G*: Western blots showing YAP/TAZ levels in FAPs treated as in *C* in the presence or absence of SB525334 (*F*) or SIS3 (*G*). *Bottom*: quantifications of TAZ expression relative to GAPDH levels. $n = 3$ independent experiments. *H*: RT-qPCR analyses showing mRNA levels of *Ankrd1* and *Ctgf* in FAPs treated as in *G*. $n = 3$ independent experiments.

genes after TGF-β stimulation. All analyzed genes (*Ankrd1*, *Cyr61*, *Ctgf*, and *Tagln2*) were markedly induced by TGF-β and entirely blocked by the addition of the Tβ-RI inhibitor SB525334, which validated a direct canonical ligand action (Fig. 3*C*). As YAP/TAZ were basally nuclear due to abundant mechanotransduction in this classic culture setting (FAPs on plastic dishes), activation of YAP/TAZ targets by TGF-β1 did not associate with a further enrichment of nuclear-localized YAP/TAZ (Fig. 3*D*). Nevertheless, TGF-β1 induced a robust upregulation of TAZ, as early as 4 h in a Tβ-RI-dependent manner (Fig. 3, *E* and *F*). To demonstrate the contribution of canonical TGF-β signaling through SMAD TFs in the activation of YAP/TAZ, we pretreated FAPs with SIS3, a specific inhibitor of SMAD3. Our results showed that SMAD inhibition completely prevents the induction of TAZ (Fig. 3*G*) and the target genes *Ankrd1* and *Ctgf* (Fig. 3*H*). Identical results of TAZ induction using SB525334 and SIS3 were found in C3H/10T1/2 in response to TGF-β, validating the use of these cells

as a FAPs model system (Supplemental Fig. S1B). All our findings support a molecular mechanism based on previous literature that SMADs are transcriptional partners of YAP/TAZ and act in concert to regulate the cellular responses of fibroblasts, with such a mechanism working similarly in FAPs (15–17, 19).

Moving in the same direction, we confirmed the connection between YAP/TAZ activation and the profibrotic nature of FAPs by surveying a published single-cell RNA-seq data set from muscles of WT, mdx, and mdxD2 mice (34) (Supplemental Fig. S2A). Previous reports described that profibrotic FAPs can be identified using omics technologies by the high expression of the cell surface molecules vascular cell adhesion molecule 1 (Vcam1) and A disintegrin and metalloprotease 12 (Adam12) (43, 44). Identification of FAPs with high levels of both markers revealed enrichment of this cell population in dystrophic muscles (Supplemental Fig. S2B). Expectedly, high levels of both YAP/TAZ and TGF-β signatures were found in Adam12 + Vcam1 + FAPs when compared with the rest of FAPs (Supplemental Fig. S2, C and D). Together, these experiments demonstrate the ability of TGF-β to activate YAP/TAZ in muscular FAPs both in vitro and in vivo.

Yap/TAZ Mechanotransduction Is Required for TGF-β-Mediated Differentiation of FAPs

Several groups have described the remarkable ability of TGF-β to induce the differentiation of fibroblasts from different tissues and organs into myofibroblasts through the activation of YAP/TAZ. Our consideration of FAPs as essentially multipotent fibroblast progenitors proposes that YAP/TAZ act in a related manner to regulate its differentiation toward the myofibroblasts phenotype, thus promoting fibrosis. We expected that in any cellular context in which YAP/TAZ is inactive, i.e., by interrupting its activity or affecting cellular mechanotransduction, TGF-β could no longer induce FAPs differentiation and consequently skeletal muscle fibrosis. To test this prediction, we first inhibited YAP/TAZ activity using the small-molecule inhibitor Verteporfin (30). Myofibroblasts are characterized by increased cell tension coupled with the induction of the smooth muscle cell-associated actin isoform α-SMA (encoded by the *Acta2* gene) and the profibrotic factor (and YAP/TAZ target) CTGF (4, 5, 28). Figure 4*A* shows that, in control conditions, all cells were already α-SMA positive, but rarely in the form of stress fibers, the key trait of contractility that defines myofibroblasts (45). Expression of α-SMA could be attributed as a process of auto "pre"-differentiation in culture due to basal YAP/TAZ activity during the growth on plastic (consistent with the protomyofibroblast phenotype) (46). Nevertheless, TGF-β was able to promote myofibroblast differentiation and the conversion of α-SMA into stress fibers, an effect that was completely blocked by Verteporfin (Fig. 4*A*). This structural feature was hand in hand with the prevention of increased *Acta2* and *Ctgf* mRNA levels (Fig. 4*B*). However, even though Verteporfin inhibits YAP/TAZ, it is known to have off-target effects (21, 47). Thus, we complemented our findings by tackling YAP/TAZ in a different manner. Cellular responses to ECM mechanics such as high extracellular stiffness, and consequently activation of YAP/TAZ, are initiated through the sensing of such physical properties by integrin receptors. Integrin binding to the ECM subsequently activates downstream signaling modules, including the focal adhesion complex and the Rho-GTPase cascade, ultimately converging on actomyosin tension (11). Since in our primary culture YAP/TAZ is basally active in the nucleus (Fig. 3*D*), we decided to inhibit the integrin downstream signaling and consequently the YAP/TAZ system through mechanotransduction by treating cells with the Rho-GTPase inhibitor C3 exotransferase or by culturing them on top of polyacrylamide (PAA) hydrogels of low stiffness (soft ECM). We validated the effectiveness of C3 and soft ECMs in preventing the accumulation of YAP/TAZ in the nucleus of C3H/10T1/2 cells (Fig. 4*C*). As expected, C3 treatment and soft ECM (this last one to a greater extent) were able to prevent TGF-β-mediated induction of *Ankrd1*, *Ctgf*, and *Acta2* (Fig. 4*D*). We replicated C3 treatment in FAPs and confirmed that interruption of cytoskeleton tension decreases the TGF-β-mediated levels of *Ctgf* and *Acta2* (Fig. 4*E*). Finally, C3 also affected the induction of TAZ and the steady-state levels of YAP (Fig. 4, *F* and *G*). Thus, our results confirm the profibrotic role of YAP/TAZ as a nuclear effector of the TGF-β profibrotic program in muscular FAPs.

Verteporfin Decreased the Extent of Skeletal Muscle Fibrosis in Mouse

To test the in vivo relevance of YAP/TAZ activation in FAPs, we switched to the inhibition of YAP/TAZ activity by Verteporfin in our fibrotic mouse model induced by G + Tβ (Fig. 2*A*). Verteporfin was administered to mice undergoing G + Tβ injection every 2 days. We found that critical fibrotic hallmarks, i.e., abundance of collagen and fibronectin, and number of FAPs (EGFP+), were limited in mice who received Verteporfin compared with vehicle-treated mice (Fig. 5, *B–D*). Reduction of fibronectin expression in mice treated with Verteporfin was also supported by Western blot of total muscle lysates (Fig. 5*E* and Supplemental Fig. S3). Finally, reduction of αSMA expression illustrates that verteporfin had interrupted the differentiation of FAPs into myofibroblasts (Fig. 5*E* and Supplemental Fig. S3). Together, these findings show the considerable role of YAP/TAZ in promoting the muscular fibrotic process by acting as nuclear effectors of TGF-β signaling.

DISCUSSION

Many reports have addressed the effective potential of YAP/TAZ to induce fibroblasts to acquire a myofibroblast phenotype in a process that affects the development and severity of tissue fibrosis across organs (20–24, 48–50). Our work provides a comprehensive description of the regulation and functionality of YAP/TAZ as elemental nuclear factors governing TGF-β responses in muscular fibroblasts, with an unprecedented spatial and single-cell resolution that sheds new light on the dynamics of this system during muscular dystrophy.

Our analyses using spatial transcriptomics (Fig. 1) suggest that the building of a complex degenerative niche of inflammatory cells, fibroblasts, and regenerative myofibers is the potential root of increased YAP/TAZ activity. Within this

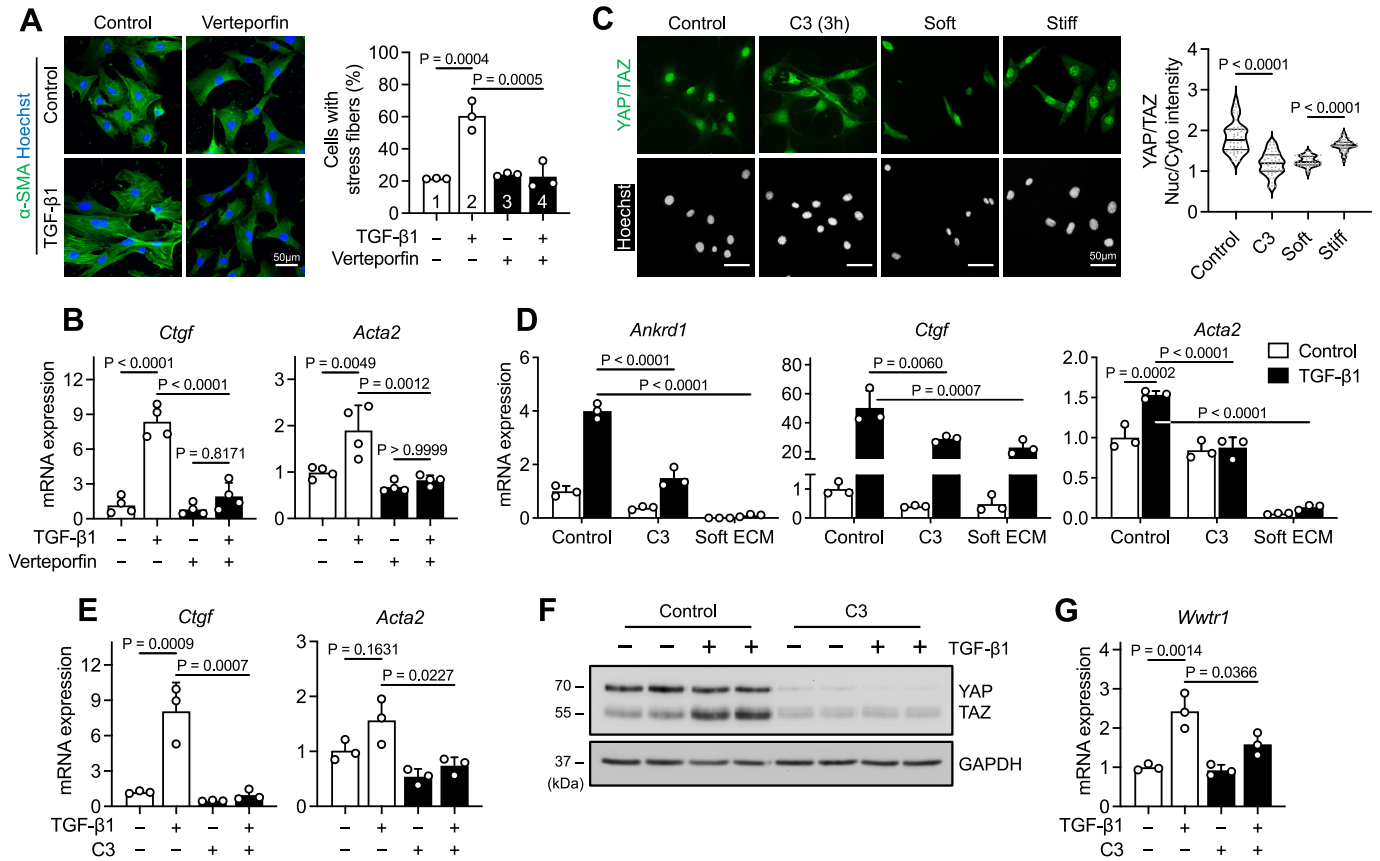

Figure 4. Inhibition of Yes-associated protein (YAP)/transcriptional coactivator with PDZ-binding motif (TAZ) affects transforming growth factor type β (TGF-β) downstream responses in fibro/adipogenic progenitors (FAPs). *A*: representative immunofluorescence images showing α-SMA signal in FAPs treated with or without 1 ng/mL TGF-β1 in the presence or absence of Verteporfin. *Right*: quantification of the percentage of cells showing stress fibers. $n = 3$ independent experiments. *B*: RT-qPCR analyses revealing mRNA levels for *Ctgf* and *Acta2* in FAPs treated as in *A*. $n = 4$ independent experiments. *C*: immunofluorescence images showing YAP/TAZ localization in C3H/10T1/2 cells treated with or without C3 exotransferase (Rho GTPase inhibitor) for 3 h or seeded on top of soft or stiff hydrogels for 24 h. *Right*: quantification of nuclear/cytoplasmic ratio of YAP/TAZ signal intensity. $n = 50$ cells in all conditions pooled from two independent experiments. *D*: RT-qPCR results showing mRNA levels for *Ankrd1*, *Ctgf*, and *Acta2* in C3H/10T1/2 cells treated with or without 1 ng/mL TGF-β1 for 6 h in the presence or absence of C3 or seeded on top of soft hydrogels. $n = 3$ independent experiments. *E*: RT-qPCR graphs showing mRNA levels of *Ctgf* and *Acta2* in FAPs treated with or without 1 ng/mL TGF-β1 for 24 h in the presence or absence of C3. $n = 3$ independent experiments. *F*: Western blot exhibiting YAP/TAZ expression in FAPs treated as in *E*. $n = 2$ independent experiments. *G*: RT-qPCR result showing mRNA levels of *Wwtr1* (TAZ) in C3H/10T1/2 cells treated as in *D*. $n = 3$ independent experiments.

context, TGF-β released from its primary cellular source, M2 macrophages, could be the starting point for YAP/TAZ activation, a cell-cell communication pair extensively described in muscular dystrophies (51). However, since YAP/TAZ, and concomitantly SMAD, activation is modulated by the physical properties of the cell environment, some questions arise about this initial phase. Is the release of TGF-β from macrophages and its subsequent exploitation by FAPs sufficient to begin a fibrotic response? And what role does the mechanical state of the muscle environment play in the very initial stages of the disease? It is worth noting that most effects of TGF-β can be experimentally muted by the inhibition of mechanotransduction, such as the use of Rho-ROCK inhibitors, soft matrices, or cell confinement (16, 21, 52–54). We expect the standard stiffness of the muscle to be a permissive starting point for the effective activation of TGF-β signaling in terms of mechanics. This hypothesis is supported by noticing that skeletal muscles exhibit a physiological stiffness of around 12 kPa (55, 56), which is far above the biological threshold for YAP/TAZ activation and saturation for most cells tested in culture settings. Recently, another group has demonstrated the nuclear localization of YAP in FAPs seeded onto biomimetic substrates of 8 kPa of stiffness (57). In vivo, we found that the majority of YAP/TAZ signal in a healthy muscle comes from the nucleus of FAPs, although at lower levels compared with fibrotic muscle (Fig. 4*C*), while others have noticed its localization in the nucleus of myofibers and interstitial cells (likely FAPs) (26). Also, other groups demonstrated that the expression of a Hippo-resistant form of YAP is sufficient to generate muscular dystrophy traits without any other insult (25, 26). This outcome is suggested to be possible only with adequate mechanotransduction since mechanical regulation of YAP/TAZ is a Hippo-independent process (12). All this evidence indicates that, in normal muscle, YAP/TAZ is mechanically active but physiologically controlled and available for an eventual profibrotic corruption initiated by extracellular signals. Indeed, these observations rely on our current technological approaches, with their limited resolution, to determine the physical properties of tissues. This matter becomes especially important when studying cells embedded

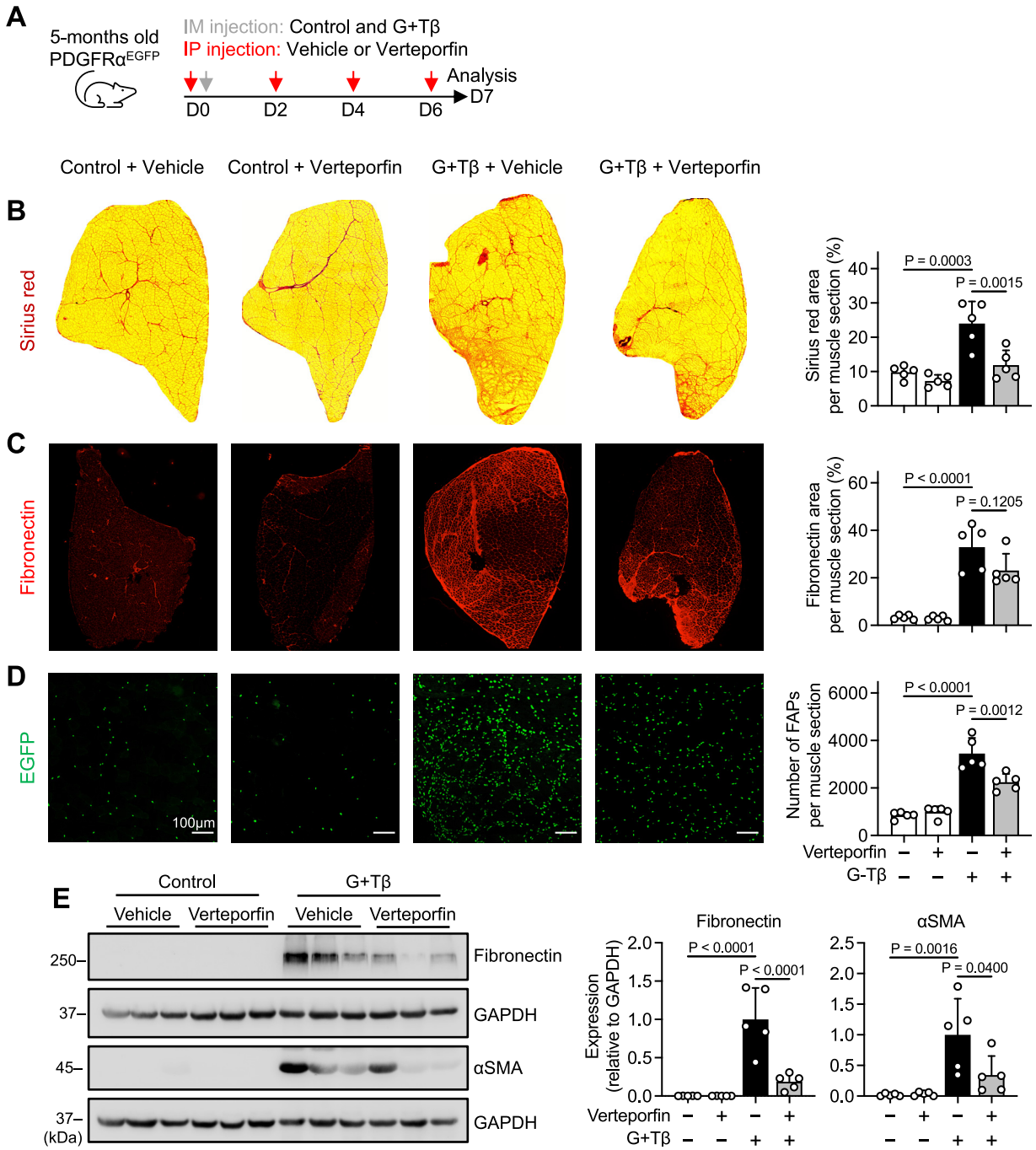

Figure 5. Skeletal muscle fibrosis is reduced in mice treated with Verteporfin. *A*: illustration indicating experimental setup for in vivo inhibition of Yes-associated protein (YAP)/transcriptional coactivator with PDZ-binding motif (TAZ) with Verteporfin. IM, intramuscular; IP, intraperitoneal; D, day. *B*: representative muscle sections showing collagen deposition by Sirius red staining. *Right*: quantification of area occupied by collagen per muscle section. *C* and *D*: representative images of fluorescence signal for enhanced green fluorescent protein (EGFP; *C*) and fibronectin (*D*). *Right*: quantification of number of fibro/adipogenic progenitors (FAPs; *C*) and area covered by fibronectin (*D*) per muscle section. *E*: Western blot analysis of fibronectin and αSMA expressions. *Right*: quantifications relative to GAPDH levels. $n = 5$ independent mice in all panels.

in such a complex architecture as the connective tissue of the skeletal muscle, which has constant deformations and stretches due to its natural function.

As initially identified and named, FAPs are characterized by having stem cell properties such as multipotency (58). Differentiation routes along the adipogenic, osteogenic, chondrogenic, fibrogenic, and even endothelial lineages have been described in this population. Here, we found that along the fibrogenic route of FAPs, there is a simultaneous increase in TAZ expression (Fig. 4). This precise induction can raise speculations for a potential function of TAZ in governing FAPs cell fate decisions. We previously showed the effective repression of the master adipogenic TF PPARγ in FAPs by TGF-β1 (40) in a manner that prevents the adipogenic conversion of these

cells. Interestingly, TAZ is a negative regulator of adipogenesis through PPARγ repression (59–62). The same attribute has been described for TEAD4 (63), although suggestively, to perform in a YAP/TAZ-independent manner. Recently, it has been described that WNT7A signaling also represses the adipogenesis of FAPs through a YAP/TAZ mechanotransduction mechanism (59). Thus, it is plausible that besides TGF-β is known to promote myofibroblast differentiation by increasing the expression of genes related to cell tension such as α-SMA, a potential parallel mechanism of concomitant repression of PPARγ suggests TAZ as a truly molecular rheostat in deciding the fibrogenic over the adipogenic route.

Our results also corroborate that YAP/TAZ activation by TGF-β is mediated by the canonical SMAD pathway (Fig. 4). This observation is supported by strong literature showing the constant interaction between YAP/TAZ and SMADs (15–19, 64). SMADs' nucleocytoplasmic shuttling and transcriptional function are predominantly governed by YAP/TAZ localization and activation (15, 16, 21). This mode of operation is associated with one of the most peculiar characteristics of SMADs: their low binding affinity with DNA on SMAD-binding elements (SBE) (9) and the requirement of partner TFs to command its genome-wide association. Indeed, gene expression programs induced by TGF-β are mainly directed by the occupancy of SMADs at the same genomic loci of cell type-specific master TFs such as Myod1 in myogenic cells (65). In the case of myofibroblasts, SMAD binding could be headed by classic TFs interacting with YAP/TAZ, such as TEADs, and by so doing, coordinating myofibroblast-specific gene expression programs associated with fibrosis. Although no consensus sequence for SBE has been observed in ChIP-seq experiments using YAP/TAZ antibodies, no data has been generated in TGF-β-treated cells (66). Therefore, whether YAP/TAZ-TEAD or YAP/TAZ interaction with other TFs controls the genomic sites of SMADs binding requires further study.

In the context of YAP/TAZ protein regulation, our work identified TGF-β as a potent inducer of TAZ expression (Fig. 3). Although this response has been observed previously, different and sometimes conflicting mechanisms have been proposed. For instance, one study suggests that a SMAD-independent pathway, involving the myocardin-related transcription factor (MRTF), drives TAZ expression (67). MRTF, a transcription factor within the serum-response factor pathway, is tightly regulated by its nuclear exclusion through interactions with monomeric G-actin, acting as a mechanotransducer. This mechanism aligns with our data showing no induction of TAZ in the presence of C3 (an indirect inhibitor of actin polymerization) (Fig. 4, *F* and *G*). Conversely, another study reports a SMAD-dependent mechanism in cancer cells (68), which supports our findings using muscular FAPs and C3H/10T1/2 cells (Fig. 3, *F* and *G* and Supplemental Fig. S2*B*). This contrasts with the results of Miranda et al. (67), where neither SMAD3 silencing nor SIS3 treatment inhibited TAZ induction in C3H/10T1/2 cells. Given that TAZ contains SBE in its promoter sequence (68), such discrepancies could potentially be attributed to differences in the fetal bovine serum used during cell culture, which might influence an unidentified molecular determinant critical for SMAD activity.

The transcriptional regulation overlap between YAP/TAZ and SMAD becomes evident by the induction of identical target genes. Indeed, some of these genes directly mediate the biological downstream effects of YAP/TAZ, as is the case of CTGF (69). CTGF is a member of the secreted extracellular CCN family of proteins intimately associated with the cell matrisome. In vivo, CTGF overexpression or blockade can trigger muscular fibrosis in a healthy mouse or prevent muscular fibrosis in a dystrophic mouse (31, 70, 71). Hence, it is highly suggestive to consider the excessive deposition of CTGF as the final product of TGF-β-YAP/TAZ association during the muscular fibrotic response.

An evident limitation of our study is the animal model used to induce fibrosis. Glycerol is an important signaling molecule in muscle cells, especially related to growth factor signaling and energy metabolism (72). Our study lacks how much glycerol affects the outcome of TGF-β in the muscular environment. However, what it is true is that, together, both molecules exert an enormous fibrotic environment suitable to recapitulate the traits of a dystrophic muscle and therefore to assess YAP/TAZ activity (39). Certainly, the use of a mouse model of muscular dystrophy (e.g., knockouts of dystrophin, dystro/sarcoglycans, *Lama2* or *Col6*) would be more translatable for muscle pathophysiology.

Overall, our work provides substantial evidence on the role of YAP/TAZ in the development of muscle degeneration associated and high TGF-β signaling activation, paving the way toward the consideration of these nuclear factors as fundamental in the fibrogenic process. It also encourages further investigation in animal models using mouse genetics or effective drugs, with high and minimal on- and off-target effects, as promising therapies (73).

DATA AVAILABILITY

Spatial and single-cell RNA-seq data used in this study are openly available at GEO under accession codes GSE225766 and GSE213925. The original articles are Refs. 33 and 34.

SUPPLEMENTAL MATERIAL

Supplemental Figs. S1–S3: https://doi.org/10.6084/m9.figshare.28182641.

ACKNOWLEDGMENTS

The authors gratefully acknowledge the FCV Animal Facility for its services and Darling Vera and Eduardo Ramírez for invaluable technical support. This work was supported by the Advanced Microscopy Facility UMA UC.

GRANTS

This study was supported by FONDECYT Grants 1190144 and 1230054, and CONICYT Grants AFB170005, AC210009, and FB210008 (to E.B.); FONDECYT Grant 1210872, ANID Grant SCIA/ACT192015, and Fondequip Grant EMQ210101 (to A.R.); Chilean National Agency for Research and Development (ANID)/Ph.D. Scholarship 21202486 and 21210650 (to F.S.G. and C.G-R.), respectively. Vicerrectoría de Investigación y Doctorados de la Universidad San Sebastián Ph.D. Scholarship 0010267181 (to J.F.-C.)

DISCLOSURES

No conflicts of interest, financial or otherwise, are declared by the authors.

AUTHOR CONTRIBUTIONS

F.S.G., A.R., and E.B. conceived and designed research; F.S.G., M.C.-S., A.B.-P., J.F.-C., C.G.-R., A.G., and V.T. performed experiments; F.S.G., M.C.-S., A.B.-P., C.G.-R., J.C.C., and E.B. analyzed data; F.S.G., M.C.-S., A.B.-P., J.F.-C., C.G.-R., J.C.C., A.R., and E.B. interpreted results of experiments; F.S.G. prepared figures; F.S.G. drafted manuscript; E.B. edited and revised manuscript; F.S.G., M.C.-S., J.F.-C., C.G.-R., A.G., V.T., J.C.C., A.R., and E.B. approved final version of manuscript.

REFERENCES

1. **Duan D**, **Goemans N**, **Takeda S**, **Mercuri E**, **Aartsma-Rus A.** Duchenne muscular dystrophy. *Nat Rev Dis Primers* 7: 13, 2021. doi:10.1038/s41572-021-00248-3.
2. **Smith LR**, **Barton ER.** Regulation of fibrosis in muscular dystrophy. *Matrix Biol* 68–69: 602–615, 2018. doi:10.1016/j.matbio.2018.01.014.
3. **Contreras O**, **Rossi FM**, **Brandan E.** Adherent muscle connective tissue fibroblasts are phenotypically and biochemically equivalent to stromal fibro/adipogenic progenitors. *Matrix Biol Plus* 2: 100006, 2019. doi:10.1016/j.mbplus.2019.04.003.
4. **Joe AW**, **Yi L**, **Natarajan A**, **Le Grand F**, **So L**, **Wang J**, **Rudnicki MA**, **Rossi FM.** Muscle injury activates resident fibro/adipogenic progenitors that facilitate myogenesis. *Nat Cell Biol* 12: 153–163, 2010. doi:10.1038/ncb2015.
5. **Uezumi A**, **Ito T**, **Morikawa D**, **Shimizu N**, **Yoneda T**, **Segawa M**, **Yamaguchi M**, **Ogawa R**, **Matev MM**, **Miyagoe-Suzuki Y**, **Takeda S**, **Tsujikawa K**, **Tsuchida K**, **Yamamoto H**, **Fukada S.** Fibrosis and adipogenesis originate from a common mesenchymal progenitor in skeletal muscle. *J Cell Sci* 124: 3654–3664, 2011. doi:10.1242/jcs.086629.
6. **Uezumi A**, **Fukada S**, **Yamamoto N**, **Ikemoto-Uezumi M**, **Nakatani M**, **Morita M**, **Yamaguchi A**, **Yamada H**, **Nishino I**, **Hamada Y**, **Tsuchida K.** Identification and characterization of PDGFRα$^+$ mesenchymal progenitors in human skeletal muscle. *Cell Death Dis* 5: e1186, 2014. doi:10.1038/cddis.2014.161.
7. **Cohn RD**, **van Erp C**, **Habashi JP**, **Soleimani AA**, **Klein EC**, **Lisi MT**, **Gamradt M**, **Ap Rhys CM**, **Holm TM**, **Loeys BL**, **Ramirez F**, **Judge DP**, **Ward CW**, **Dietz HC.** Angiotensin II type 1 receptor blockade attenuates TGF-β-induced failure of muscle regeneration in multiple myopathic states. *Nat Med* 13: 204–210, 2007 [Erratum in *Nat Med* 13: 511, 2007]. doi:10.1038/nm1536.
8. **Kemaladewi DU**, **Pasteuning S**, **van der Meulen JW**, **van Heiningen SH**, **van Ommen GJ**, **Ten Dijke P**, **Aartsma-Rus A**, **'t Hoen PA**, **Hoogaars WM.** Targeting TGF-β signaling by antisense oligonucleotide-mediated knockdown of TGF-β type I receptor. *Mol Ther Nucleic Acids* 3: e156, 2014. doi:10.1038/mtna.2014.7.
9. **Massague J**, **Seoane J**, **Wotton D.** Smad transcription factors. *Genes Dev* 19: 2783–2810, 2005. doi:10.1101/gad.1350705.
10. **Piersma B**, **Bank RA**, **Boersema M.** Signaling in fibrosis: TGF-β, WNT, and YAP/TAZ converge. *Front Med (Lausanne)* 2: 59, 2015. doi:10.3389/fmed.2015.00059.
11. **Totaro A**, **Panciera T**, **Piccolo S.** YAP/TAZ upstream signals and downstream responses. *Nat Cell Biol* 20: 888–899, 2018. doi:10.1038/s41556-018-0142-z.
12. **Dupont S**, **Morsut L**, **Aragona M**, **Enzo E**, **Giulitti S**, **Cordenonsi M**, **Zanconato F**, **Le Digabel J**, **Forcato M**, **Bicciato S**, **Elvassore N**, **Piccolo S.** Role of YAP/TAZ in mechanotransduction. *Nature* 474: 179–183, 2011. doi:10.1038/nature10137.
13. **Elosegui-Artola A**, **Andreu I**, **Beedle AEM**, **Lezamiz A**, **Uroz M**, **Kosmalska AJ**, **Oria R**, **Kechagia JZ**, **Rico-Lastres P**, **Le Roux AL**, **Shanahan CM**, **Trepat X**, **Navajas D**, **Garcia-Manyes S**, **Roca-Cusachs P.** Force triggers YAP nuclear entry by regulating transport across nuclear pores. *Cell* 171: 1397–1410.e14, 2017. doi:10.1016/j.cell.2017.10.008.
14. **Aragona M**, **Panciera T**, **Manfrin A**, **Giulitti S**, **Michielin F**, **Elvassore N**, **Dupont S**, **Piccolo S.** A mechanical checkpoint controls multicellular growth through YAP/TAZ regulation by actin-processing factors. *Cell* 154: 1047–1059, 2013. doi:10.1016/j.cell.2013.07.042.
15. **Varelas X**, **Sakuma R**, **Samavarchi-Tehrani P**, **Peerani R**, **Rao BM**, **Dembowy J**, **Yaffe MB**, **Zandstra PW**, **Wrana JL.** TAZ controls Smad nucleocytoplasmic shuttling and regulates human embryonic stem-cell self-renewal. *Nat Cell Biol* 10: 837–848, 2008. doi:10.1038/ncb1748.
16. **Varelas X**, **Samavarchi-Tehrani P**, **Narimatsu M**, **Weiss A**, **Cockburn K**, **Larsen BG**, **Rossant J**, **Wrana JL.** The Crumbs complex couples cell density sensing to Hippo-dependent control of the TGF-β-SMAD pathway. *Dev Cell* 19: 831–844, 2010. doi:10.1016/j.devcel.2010.11.012.
17. **Hiemer SE**, **Szymaniak AD**, **Varelas X.** The transcriptional regulators TAZ and YAP direct transforming growth factor β-induced tumorigenic phenotypes in breast cancer cells. *J Biol Chem* 289: 13461–13474, 2014. doi:10.1074/jbc.M113.529115.
18. **Pefani DE**, **Pankova D**, **Abraham AG**, **Grawenda AM**, **Vlahov N**, **Scrace S**, **O' Neil E.** TGF-β targets the hippo pathway scaffold RASSF1A to facilitate YAP/SMAD2 nuclear translocation. *Mol Cell* 63: 156–166, 2016. doi:10.1016/j.molcel.2016.05.012.
19. **Wang Y**, **Tu K**, **Liu D**, **Guo L**, **Chen Y**, **Li Q**, **Maiers JL**, **Liu Z**, **Shah VH**, **Dou C**, **Tschumperlin D**, **Voneschen L**, **Yang R**, **Kang N.** p300 acetyltransferase is a cytoplasm-to-nucleus shuttle for SMAD2/3 and TAZ nuclear transport in transforming growth factor β-stimulated hepatic stellate cells. *Hepatology* 70: 1409–1423, 2019. doi:10.1002/hep.30668.
20. **Liu F**, **Lagares D**, **Choi KM**, **Stopfer L**, **Marinkovic A**, **Vrbanac V**, **Probst CK**, **Hiemer SE**, **Sisson TH**, **Horowitz JC**, **Rosas IO**, **Fredenburgh LE**, **Feghali-Bostwick C**, **Varelas X**, **Tager AM**, **Tschumperlin DJ.** Mechanosignaling through YAP and TAZ drives fibroblast activation and fibrosis. *Am J Physiol Lung Cell Mol Physiol* 308: L344–L357, 2015. doi:10.1152/ajplung.00300.2014.
21. **Szeto SG**, **Narimatsu M**, **Lu M**, **He X**, **Sidiqi AM**, **Tolosa MF**, **Chan L**, **De Freitas K**, **Bialik JF**, **Majumder S**, **Boo S**, **Hinz B**, **Dan Q**, **Advani A**, **John R**, **Wrana JL**, **Kapus A**, **Yuen DA.** YAP/TAZ are mechanoregulators of TGF-β-Smad signaling and renal fibrogenesis. *J Am Soc Nephrol* 27: 3117–3128, 2016. doi:10.1681/ASN.2015050499.
22. **Mia MM**, **Cibi DM**, **Ghani S**, **Singh A**, **Tee N**, **Sivakumar V**, **Bogireddi H**, **Cook SA**, **Mao J**, **Singh MK.** Loss of Yap/Taz in cardiac fibroblasts attenuates adverse remodelling and improves cardiac function. *Cardiovasc Res* 118: 1785–1804, 2022. doi:10.1093/cvr/cvab205.
23. **Piersma B**, **de Rond S**, **Werker PM**, **Boo S**, **Hinz B**, **van Beuge MM**, **Bank RA.** YAP1 is a driver of myofibroblast differentiation in normal and diseased fibroblasts. *Am J Pathol* 185: 3326–3337, 2015. doi:10.1016/j.ajpath.2015.08.011.
24. **Shi-Wen X**, **Racanelli M**, **Ali A**, **Simon A**, **Quesnel K**, **Stratton RJ**, **Leask A.** Verteporfin inhibits the persistent fibrotic phenotype of lesional scleroderma dermal fibroblasts. *J Cell Commun Signal* 15: 71–80, 2021. doi:10.1007/s12079-020-00596-x.
25. **Judson RN**, **Gray SR**, **Walker C**, **Carroll AM**, **Itzstein C**, **Lionikas A**, **Zammit PS**, **De Bari C**, **Wackerhage H.** Constitutive expression of Yes-associated protein (Yap) in adult skeletal muscle fibres induces muscle atrophy and myopathy. *PLoS One* 8: e59622, 2013. doi:10.1371/journal.pone.0059622.
26. **Watt KI**, **Turner BJ**, **Hagg A**, **Zhang X**, **Davey JR**, **Qian H**, **Beyer C**, **Winbanks CE**, **Harvey KF**, **Gregorevic P.** The Hippo pathway effector YAP is a critical regulator of skeletal muscle fibre size. *Nat Commun* 6: 6048, 2015. doi:10.1038/ncomms7048.
27. **Gallardo FS**, **Córdova-Casanova A**, **Bock-Pereda A**, **Rebolledo DL**, **Ravasio A**, **Casar JC**, **Brandan E.** Denervation drives YAP/TAZ activation in muscular fibro/adipogenic progenitors. *Int J Mol Sci* 24: 5585, 2023. doi:10.3390/ijms24065585.
28. **Cruz-Soca M**, **Faundez-Contreras J**, **Córdova-Casanova A**, **Gallardo FS**, **Bock-Pereda A**, **Chun J**, **Casar JC**, **Brandan E.** Activation of skeletal muscle FAPs by LPA requires the Hippo signaling via the FAK pathway. *Matrix Biol* 119: 57–81, 2023. doi:10.1016/j.matbio.2023.03.010.
29. **Hamilton TG**, **Klinghoffer RA**, **Corrin PD**, **Soriano P.** Evolutionary divergence of platelet-derived growth factor α receptor signaling mechanisms. *Mol Cell Biol* 23: 4013–4025, 2003. doi:10.1128/MCB.23.11.4013-4025.2003.

30. **Liu-Chittenden Y**, **Huang B**, **Shim JS**, **Chen Q**, **Lee SJ**, **Anders RA**, **Liu JO**, **Pan D.** Genetic and pharmacological disruption of the TEAD-YAP complex suppresses the oncogenic activity of YAP. *Genes Dev* 26: 1300–1305, 2012. doi:10.1101/gad.192856.112.
31. **Rebolledo DL**, **González D**, **Faundez-Contreras J**, **Contreras O**, **Vio CP**, **Murphy-Ullrich JE**, **Lipson KE**, **Brandan E.** Denervation-induced skeletal muscle fibrosis is mediated by CTGF/CCN2 independently of TGF-β. *Matrix Biol* 82: 20–37, 2019. doi:10.1016/j.matbio.2019.01.002.
32. **Gandin A**, **Torresan V**, **Ulliana L**, **Panciera T**, **Contessotto P**, **Citron A**, **Zanconato F**, **Cordenonsi M**, **Piccolo S**, **Brusatin G.** Broadly applicable hydrogel fabrication procedures guided by YAP/TAZ-activity reveal stiffness, adhesiveness, and nuclear projected area as checkpoints for mechanosensing. *Adv Healthc Mater* 11: e2102276, 2022. doi:10.1002/adhm.202102276.
33. **Stec MJ**, **Su Q**, **Adler C**, **Zhang L**, **Golann DR**, **Khan NP**, **Panagis L**, **Villalta SA**, **Ni M**, **Wei Y**, **Walls JR**, **Murphy AJ**, **Yancopoulos GD**, **Atwal GS**, **Kleiner S**, **Halasz G**, **Sleeman MW.** A cellular and molecular spatial atlas of dystrophic muscle. *Proc Natl Acad Sci USA* 120: e2221249120, 2023. doi:10.1073/pnas.2221249120.
34. **Saleh KK**, **Xi H**, **Switzler C**, **Skuratovsky E**, **Romero MA**, **Chien P**, **Gibbs D**, **Gane L**, **Hicks MR**, **Spencer MJ**, **Pyle AD.** Single cell sequencing maps skeletal muscle cellular diversity as disease severity increases in dystrophic mouse models. *iScience* 25: 105415, 2022. doi:10.1016/j.isci.2022.105415.
35. **Alsamman S**, **Christenson SA**, **Yu A**, **Ayad NME**, **Mooring MS**, **Segal JM**, **Hu JK**, **Schaub JR**, **Ho SS**, **Rao V**, **Marlow MM**, **Turner SM**, **Sedki M**, **Pantano L**, **Ghoshal S**, **Ferreira DDS**, **Ma HY**, **Duwaerts CC**, **Espanol-Suner R**, **Wei L**, **Newcomb B**, **Mileva I**, **Canals D**, **Hannun YA**, **Chung RT**, **Mattis AN**, **Fuchs BC**, **Tager AM**, **Yimlamai D**, **Weaver VM**, **Mullen AC**, **Sheppard D**, **Chen JY.** Targeting acid ceramidase inhibits YAP/TAZ signaling to reduce fibrosis in mice. *Sci Transl Med* 12: eaay8798, 2020. doi:10.1126/scitranslmed.aay8798.
36. **Padua D**, **Zhang XH**, **Wang Q**, **Nadal C**, **Gerald WL**, **Gomis RR**, **Massagué J.** TGFβ primes breast tumors for lung metastasis seeding through angiopoietin-like 4. *Cell* 133: 66–77, 2008. doi:10.1016/j.cell.2008.01.046.
37. **Vita GL**, **Polito F**, **Oteri R**, **Arrigo R**, **Ciranni AM**, **Musumeci O**, **Messina S**, **Rodolico C**, **Di Giorgio RM**, **Vita G**, **Aguennouz M.** Hippo signaling pathway is altered in Duchenne muscular dystrophy. *PLoS One* 13: e0205514, 2018. doi:10.1371/journal.pone.0205514.
38. **Morales MG**, **Acuña MJ**, **Cabrera D**, **Goldschmeding R**, **Brandan E.** The pro-fibrotic connective tissue growth factor (CTGF/CCN2) correlates with the number of necrotic-regenerative foci in dystrophic muscle. *J Cell Commun Signal* 12: 413–421, 2018. doi:10.1007/s12079-017-0409-3.
39. **Mahdy MAA**, **Warita K**, **Hosaka YZ.** Effects of transforming growth factor-β1 treatment on muscle regeneration and adipogenesis in glycerol-injured muscle. *Anim Sci J* 88: 1811–1819, 2017. doi:10.1111/asj.12845.
40. **Contreras O**, **Cruz-Soca M**, **Theret M**, **Soliman H**, **Tung LW**, **Groppa E**, **Rossi FM**, **Brandan E.** Cross-talk between TGF-β and PDGFRα signaling pathways regulates the fate of stromal fibro-adipogenic progenitors. *J Cell Sci* 132: jcs232157, 2019. doi:10.1242/jcs.232157.
41. **Mathew SJ**, **Hansen JM**, **Merrell AJ**, **Murphy MM**, **Lawson JA**, **Hutcheson DA**, **Hansen MS**, **Angus-Hill M**, **Kardon G.** Connective tissue fibroblasts and Tcf4 regulate myogenesis. *Development* 138: 371–384, 2011. doi:10.1242/dev.057463.
42. **Contreras O**, **Soliman H**, **Theret M**, **Rossi FMV**, **Brandan E.** TGF-β-driven downregulation of the transcription factor TCF7L2 affects Wnt/β-catenin signaling in PDGFRα$^+$ fibroblasts. *J Cell Sci* 133: jcs242297, 2020. doi:10.1242/jcs.242297.
43. **Dulauroy S**, **Di Carlo SE**, **Langa F**, **Eberl G**, **Peduto L.** Lineage tracing and genetic ablation of ADAM12$^+$ perivascular cells identify a major source of profibrotic cells during acute tissue injury. *Nat Med* 18: 1262–1270, 2012. doi:10.1038/nm.2848.
44. **Malecova B**, **Gatto S**, **Etxaniz U**, **Passafaro M**, **Cortez A**, **Nicoletti C**, **Giordani L**, **Torcinaro A**, **De Bardi M**, **Bicciato S**, **De Santa F**, **Madaro L**, **Puri PL.** Dynamics of cellular states of fibro-adipogenic progenitors during myogenesis and muscular dystrophy. *Nat Commun* 9: 3670, 2018. doi:10.1038/s41467-018-06068-6.
45. **Younesi FS**, **Miller AE**, **Barker TH**, **Rossi FMV**, **Hinz B.** Fibroblast and myofibroblast activation in normal tissue repair and fibrosis. *Nat Rev Mol Cell Biol* 25: 617–638, 2024. [Erratum in *Nat Rev Mol Cell Biol* 25: 671, 2024]. doi:10.1038/s41580-024-00716-0.
46. **Son DO**, **Benitez R**, **Diao L**, **Hinz B.** How to keep myofibroblasts under control: culture of mouse skin fibroblasts on soft substrates. *J Invest Dermatol* 144: 1923–1934, 2024. doi:10.1016/j.jid.2024.05.033.
47. **Dey A**, **Varelas X**, **Guan KL.** Targeting the Hippo pathway in cancer, fibrosis, wound healing and regenerative medicine. *Nat Rev Drug Discov* 19: 480–494, 2020. doi:10.1038/s41573-020-0070-z.
48. **Mannaerts I**, **Leite SB**, **Verhulst S**, **Claerhout S**, **Eysackers N**, **Thoen LF**, **Hoorens A**, **Reynaert H**, **Halder G**, **van Grunsven LA.** The Hippo pathway effector YAP controls mouse hepatic stellate cell activation. *J Hepatol* 63: 679–688, 2015. doi:10.1016/j.jhep.2015.04.011.
49. **Liang M**, **Yu M**, **Xia R**, **Song K**, **Wang J**, **Luo J**, **Chen G**, **Cheng J.** Yap/Taz deletion in Gli$^+$ cell-derived myofibroblasts attenuates fibrosis. *J Am Soc Nephrol* 28: 3278–3290, 2017. doi:10.1681/ASN.2015121354.
50. **Garoffolo G**, **Casaburo M**, **Amadeo F**, **Salvi M**, **Bernava G**, **Piacentini L**, **Chimenti I**, **Zaccagnini G**, **Milcovich G**, **Zuccolo E**, **Agrifoglio M**, **Ragazzini S**, **Baasansuren O**, **Cozzolino C**, **Chiesa M**, **Ferrari S**, **Carbonaro D**, **Santoro R**, **Manzoni M**, **Casalis L**, **Raucci A**, **Molinari F**, **Menicanti L**, **Pagano F**, **Ohashi T**, **Martelli F**, **Massai D**, **Colombo GI**, **Messina E**, **Morbiducci U**, **Pesce M.** Reduction of cardiac fibrosis by interference with YAP-dependent transactivation. *Circ Res* 131: 239–257, 2022. doi:10.1161/CIRCRESAHA.121.319373.
51. **Tidball JG**, **Welc SS**, **Wehling-Henricks M.** Immunobiology of inherited muscular dystrophies. *Compr Physiol* 8: 1313–1356, 2018. doi:10.1002/cphy.c170052.
52. **Pitha I**, **Oglesby E**, **Chow A**, **Kimball E**, **Pease ME**, **Schaub J**, **Quigley H.** Rho-kinase inhibition reduces myofibroblast differentiation and proliferation of scleral fibroblasts induced by transforming growth factor β and experimental glaucoma. *Transl Vis Sci Technol* 7: 6, 2018. doi:10.1167/tvst.7.6.6.
53. **Futakuchi A**, **Inoue T**, **Fujimoto T**, **Inoue-Mochita M**, **Kawai M**, **Tanihara H.** The effects of ripasudil (K-115), a Rho kinase inhibitor, on activation of human conjunctival fibroblasts. *Exp Eye Res* 149: 107–115, 2016. doi:10.1016/j.exer.2016.07.001.
54. **Nagatoya K**, **Moriyama T**, **Kawada N**, **Takeji M**, **Oseto S**, **Murozono T**, **Ando A**, **Imai E**, **Hori M.** Y-27632 prevents tubulointerstitial fibrosis in mouse kidneys with unilateral ureteral obstruction. *Kidney Int* 61: 1684–1695, 2002. doi:10.1046/j.1523-1755.2002.00328.x.
55. **Engler AJ**, **Griffin MA**, **Sen S**, **Bonnemann CG**, **Sweeney HL**, **Discher DE.** Myotubes differentiate optimally on substrates with tissue-like stiffness: pathological implications for soft or stiff microenvironments. *J Cell Biol* 166: 877–887, 2004. doi:10.1083/jcb.200405004.
56. **Smith L**, **Cho S**, **Discher DE.** Mechanosensing of matrix by stem cells: from matrix heterogeneity, contractility, and the nucleus in pore-migration to cardiogenesis and muscle stem cells in vivo. *Semin Cell Dev Biol* 71: 84–98, 2017. doi:10.1016/j.semcdb.2017.05.025.
57. **Loomis T**, **Hu LY**, **Wohlgemuth RP**, **Chellakudam RR**, **Muralidharan PD**, **Smith LR.** Matrix stiffness and architecture drive fibro-adipogenic progenitors' activation into myofibroblasts. *Sci Rep* 12: 13582, 2022. doi:10.1038/s41598-022-17852-2.
58. **Soliman H**, **Theret M**, **Scott W**, **Hill L**, **Underhill TM**, **Hinz B**, **Rossi FMV.** Multipotent stromal cells: one name, multiple identities. *Cell Stem Cell* 28: 1690–1707, 2021. doi:10.1016/j.stem.2021.09.001.
59. **Fu C**, **Chin-Young B**, **Park G**, **Guzmán-Seda M**, **Laudier D**, **Han WM.** WNT7A suppresses adipogenesis of skeletal muscle mesenchymal stem cells and fatty infiltration through the alternative Wnt-Rho-YAP/TAZ signaling axis. *Stem Cell Reports* 18: 999–1014, 2023. doi:10.1016/j.stemcr.2023.03.001.
60. **El Ouarrat D**, **Isaac R**, **Lee YS**, **Oh DY**, **Wollam J**, **Lackey D**, **Riopel M**, **Bandyopadhyay G**, **Seo JB**, **Sampath-Kumar R**, **Olefsky JM.** TAZ is a negative regulator of PPARγ activity in adipocytes and TAZ deletion improves insulin sensitivity and glucose tolerance. *Cell Metab* 31: 162–173.e5, 2020. doi:10.1016/j.cmet.2019.10.003.
61. **Hong JH**, **Hwang ES**, **McManus MT**, **Amsterdam A**, **Tian Y**, **Kalmukova R**, **Mueller E**, **Benjamin T**, **Spiegelman BM**, **Sharp PA**, **Hopkins N**, **Yaffe MB.** TAZ, a transcriptional modulator of mesenchymal stem cell differentiation. *Science* 309: 1074–1078, 2005. doi:10.1126/science.1110955.

62. **Shen H**, **Huang X**, **Zhao Y**, **Wu D**, **Xue K**, **Yao J**, **Wang Y**, **Tang N**, **Qiu Y.** The Hippo pathway links adipocyte plasticity to adipose tissue fibrosis. *Nat Commun* 13: 6030, 2022. doi:10.1038/s41467-022-33800-0.
63. **Zhang W**, **Xu J**, **Li J**, **Guo T**, **Jiang D**, **Feng X**, **Ma X**, **He L**, **Wu W**, **Yin M**, **Ge L**, **Wang Z**, **Ho MS**, **Zhao Y**, **Fei Z**, **Zhang L.** The TEA domain family transcription factor TEAD4 represses murine adipogenesis by recruiting the cofactors VGLL4 and CtBP2 into a transcriptional complex. *J Biol Chem* 293: 17119–17134, 2018. doi:10.1074/jbc.RA118.003608.
64. **Labibi B**, **Bashkurov M**, **Wrana JL**, **Attisano L.** Modeling the control of TGF-β/Smad nuclear accumulation by the Hippo pathway effectors, Taz/Yap. *iScience* 23: 101416, 2020. doi:10.1016/j.isci.2020.101416.
65. **Mullen AC**, **Orlando DA**, **Newman JJ**, **Lovén J**, **Kumar RM**, **Bilodeau S**, **Reddy J**, **Guenther MG**, **DeKoter RP**, **Young RA.** Master transcription factors determine cell-type-specific responses to TGF-β signaling. *Cell* 147: 565–576, 2011. doi:10.1016/j.cell.2011.08.050.
66. **Battilana G**, **Zanconato F**, **Piccolo S.** Mechanisms of YAP/TAZ transcriptional control. *Cell Stress* 5: 167–172, 2021. doi:10.15698/cst2021.11.258.
67. **Miranda MZ**, **Bialik JF**, **Speight P**, **Dan Q**, **Yeung T**, **Szaszi K**, **Pedersen SF**, **Kapus A.** TGF-β1 regulates the expression and transcriptional activity of TAZ protein via a Smad3-independent, myocardin-related transcription factor-mediated mechanism. *J Biol Chem* 292: 14902–14920, 2017. doi:10.1074/jbc.M117.780502.
68. **Rios-López DG**, **Tecalco-Cruz AC**, **Martínez-Pastor D**, **Sosa-Garrocho M**, **Tapia-Urzúa G**, **Aranda-Lopez Y**, **Ortega-Domínguez B**, **Recillas-Targa F**, **Vázquez-Victorio G**, **Macías-Silva M.** TGF-β/SMAD canonical pathway induces the expression of transcriptional cofactor TAZ in liver cancer cells. *Heliyon* 9: e21519, 2023. doi:10.1016/j.heliyon.2023.e21519.
69. **Zhao B**, **Ye X**, **Yu J**, **Li L**, **Li W**, **Li S**, **Yu J**, **Lin JD**, **Wang CY**, **Chinnaiyan AM**, **Lai ZC**, **Guan KL.** TEAD mediates YAP-dependent gene induction and growth control. *Genes Dev* 22: 1962–1971, 2008. doi:10.1101/gad.1664408.
70. **Morales MG**, **Cabello-Verrugio C**, **Santander C**, **Cabrera D**, **Goldschmeding R**, **Brandan E.** CTGF/CCN-2 over-expression can directly induce features of skeletal muscle dystrophy. *J Pathol* 225: 490–501, 2011. doi:10.1002/path.2952.
71. **Morales MG**, **Gutierrez J**, **Cabello-Verrugio C**, **Cabrera D**, **Lipson KE**, **Goldschmeding R**, **Brandan E.** Reducing CTGF/CCN2 slows down mdx muscle dystrophy and improves cell therapy. *Hum Mol Genet* 22: 4938–4951, 2013. doi:10.1093/hmg/ddt352.
72. **Rahib L**, **Sriram G**, **Harada MK**, **Liao JC**, **Dipple KM.** Transcriptomic and network component analysis of glycerol kinase in skeletal muscle using a mouse model of glycerol kinase deficiency. *Mol Genet Metab* 96: 106–112, 2009. doi:10.1016/j.ymgme.2008.11.163.
73. **Chapeau EA**, **Sansregret L**, **Galli GG**, **Chène P**, **Wartmann M**, **Mourikis TP**, **Jaaks P**, **Baltschukat S**, **Barbosa IAM**, **Bauer D**, **Brachmann SM**, **Delaunay C**, **Estadieu C**, **Faris JE**, **Furet P**, **Harlfinger S**, **Hueber A**, **Jiménez Núñez E**, **Kodack DP**, **Mandon E**, **Martin T**, **Mesrouze Y**, **Romanet V**, **Scheufler C**, **Sellner H**, **Stamm C**, **Sterker D**, **Tordella L**, **Hofmann F**, **Soldermann N**, **Schmelzle T.** Direct and selective pharmacological disruption of the YAP-TEAD interface by IAG933 inhibits Hippo-dependent and RAS-MAPK-altered cancers. *Nat Cancer* 5: 1130, 2024. doi:10.1038/s43018-024-00797-y.